Journal of Power Sources 256 (2014) 183–189

Contents lists available at ScienceDirect

Journal of Power Sources

journal homepage: www.elsevier.com/locate/jpowsour

A method of determining interface methanol concentration in an operating direct methanol fuel cell

Jiahua Han [a], Hongtan Liu [b,*]

[a] School of Manufacturing Science and Engineering, Sichuan University, Chengdu, Sichuan 610065, People's Republic of China
[b] Clean Energy Research Institute, Department of Mechanical and Aerospace Engineering, University of Miami, Coral Gables, FL 33124, USA

HIGHLIGHTS

- Formation of peaks and valleys in methanol crossover flux are analyzed.
- Developed a novel method to determine interfacial methanol concentration.
- Methanol drag coefficient is obtained from these peaks and valleys.
- Water drag coefficient can also be obtained from these peaks and valleys.

ARTICLE INFO

Article history:
Received 13 November 2013
Received in revised form
9 January 2014
Accepted 10 January 2014
Available online 21 January 2014

Keywords:
Interface methanol concentration
Methanol drag coefficient
methanol cross-over
DMFC

ABSTRACT

Methanol crossover is a serious problem for a direct methanol fuel cell (DMFC) since it causes mixed potential and waste of fuel. The amount of methanol crossover directly depends on the methanol concentration at the interface between the anode catalyst layer and the electrolyte membrane. However, no technique is available to measure the methanol concentration at this interface in an operating DMFC. Previous experimental results show that sharp peaks exist in the methanol crossover flux when the cell voltage changes abruptly [1]. Systematic studies on these peaks reveal the formation mechanisms. Furthermore, a novel method to determine the methanol concentration at the interface between the anode catalyst layer and the Nafion® electrolyte membrane is developed. Finally, the relationship between the methanol concentration at this interface and the drag coefficients for methanol and water in an operating DMFC are also derived.

1. Introduction

Direct methanol fuel cell (DMFC) is a promising energy conversion device for portable electronics because of its low working temperature, independence of power grid, quick refueling, compact size, etc [2–4]. Furthermore, methanol fuel is a promising alternative to petroleum-based fuels since it is less expensive to produce sustainably and its use is an inexpensive way to reduce carbon footprints. Compared with hydrogen PEM fuel cells, a DMFC does not require humidification since the liquid methanol in the anode and the water produced in the cathode are sufficient to keep the Nafion® membrane well hydrated. Despite all these advantages, there are several hurdles that prevent DMFCs from being competitive to existing power systems. One of the most serious hurdles is the methanol crossover. Narayanan et al. [5] reported that over 40% of methanol could be wasted due to cross-over through thinner Nafion® membranes.

Methanol crossover happens when methanol molecules move through the electrolyte membrane from the anode side to the cathode side. It has a serious detrimental effect on cell performance due to the adverse effect caused by the formation of mixed potentials at the cathode. Methanol crossover also reduces fuel efficiency of the cell as the oxidation of the crossed-over methanol does not generate any electrical power. Though the efficiency of a DMFC stack is highly dependent upon the operating conditions as well as the cell and system configurations [6], of the total chemical energy contained in methanol, less than 30% can be converted into electricity, with the rest being converted into heat as the results of methanol crossover and the irreversibility of electrode reactions, especially in the anode [2]. Although pure methanol has a high energy density (about 1.8 kWh kg^{-1} or 1.7 kWh L^{-1}), in order to mitigate the adverse effect of methanol crossover, generally pure methanol has to be diluted to a low concentration [2] before being supplied to an operating DMFC. However, the consequence of

* Corresponding author. Tel.: +1 3052842019; fax: +1 3052842580.
E-mail address: hliu@miami.edu (H. Liu).

0378-7753/$ – see front matter © 2014 Elsevier B.V. All rights reserved.
http://dx.doi.org/10.1016/j.jpowsour.2014.01.048

dilution is that the size of the fuel cell system has to be increased significantly. Thus potential for applications of DMFCs as power sources for portable electronic devices are dramatically reduced. Another adverse effect of methanol crossover is its effect on the kinetics of the electro-reduction of oxygen at the cathode side [2]. Though the rate of reactions can be increased by increase either anode and/or cathode catalyst [7], however increasing catalysts will leads to increases in cost.

One way to reduce the methanol crossover is to use an electrolyte membrane that resist to methanol crossover. SPEEK (sulfonated poly(ether ether ketone)) and PVA (poly(vinyl alcohol)) are considered as two of the most promising candidates for replacing Nafion® electrolyte member [8–10]. Other double layer and multilayer membranes are also developed to suppress methanol crossover in a DMFC [11]. Numerous efforts have also been focused on composite membranes [12,13] to reduce the methanol crossover. Modified Nafion® membranes have also been used to improve the performance of DMFCs [14]. Omosebi and Besser [15] studied Patterned Nafion® 212 membrane prepared by electron beam lithography (EBL) coupled with dry etching. Yamauchi et al. [16] used a pore-filling polymer electrolyte membrane. Wang et al. [17] concluded that a facile surface modification of Nafion® membrane by the formation of self-polymerized dopamine nano-layer is beneficial to enhance the methanol barrier property. Li et al. [18] use stainless steel fiber felt as cathode diffusion backing and current collector for a micro direct methanol fuel cell with low methanol crossover.

Methanol crossover and its detrimental effects can also be mitigated by working on many other aspects of a DMFC. Dedicated efforts on studying new kind of the cathode electrode structure [19], modified anode [20], and the influence of the diffusion layer on methanol crossover [21] have also be conducted to reduce methanol crossover. Numerous efforts also have been made on vapor-fed DMFC in order to lower the methanol crossover and improve the cell performance [22]. Yuan et al. [23] used a porous metal-fiber sintered plate (PMFSP) based on multi-tooth cutting and high-temperature solid-phase sintering as a methanol barrier at the anode of a passive DMFC in order to reduce the effect of methanol crossover. Kim et al. [24] investigated the effects of the microstructure and powder compositions for the micro-porous layer (MPL) of an anode on the cell performance and methanol crossover. Other efforts, such as developing methanol-tolerant cathode catalysts for DMFCs [25,26] etc. have also been made. However, methanol crossover from the anode to the cathode is unavoidable despite of all the efforts from various aspects, since methanol can be dissolved into water to any degree.

Methanol crossover in a DMFC includes three parts, diffusion, electro-osmotic drag (EOD) and hydraulic permeation. Diffusion takes place due to concentration gradients across the membrane, hydraulic permeation is caused by pressure gradients, and EOD is caused by proton drag on water and methanol is dissolved in water [27]. Each part is directly proportional to the methanol concentration at the interface between the anode catalyst layer and the electrolyte membrane. Measurement of the interface methanol concentration can facilitate our understanding the roles of methanol crossover due to different mechanisms and may thus lead to development of membranes with higher resistance to methanol crossover. Some researches toward this goal have been conducted. For instance, Zhong et al. [28] evaluated the crosslinked suffocated poly (ether ether ketone)/2-acrylamido-2-methyl-1-propanesulfonic acid (SPEEK/AMPS) blend membranes and they found that the proton conductivity and methanol diffusion coefficient of SPEEK/AMPS membranes increased gradually with the increase of AMPS content. Another study by Zhong et al. [29] found that the existence of self-cross linked silica network of organic/inorganic proton exchange membranes enable them to possess excellent thermal stability and methanol barrier. Baglio et al. [30] studied water and methanol transport properties through bare recast Nafion® and composite Nafion® membranes containing ceramic fillers characterized by different acid–base behavior. In their study, both nuclear magnetic resonance (NMR) and electro-chemical polarization data indicate that both electrical properties and transport mechanism are influenced by the surface properties of the inorganic fillers.

Methanol concentration at the interface between the anode catalyst layer and the membrane is also related to the reaction kinetics in the anode catalyst layer. A higher methanol oxidation rate leads to a lower interfacial methanol concentration. Numerous papers have been published on studying the effects of methanol crossover [31], the mechanisms of methanol crossover [27], methods to mitigate the methanol crossover, the effects of different operating conditions on the methanol crossover [1,33], either experimentally or numerically. Seo and Lee [31] found that the efficiency of a DMFC is directly related to the methanol crossover during operation. Arico et al. [32] found that methanol crossover can reduce the open-circuit potential by as much as 0.15–0.2 V and poison the catalysts at the cathode. Han and Liu [1] measured methanol crossover in an operating fuel cell under different operating conditions. Chiu [33] evaluated methanol crossover in a DMFC under different operating conditions with an algebraic semi-empirical model. However, a method to measure the methanol concentration at the interface between the anode catalyst layer and the electrolyte membrane is still elusive, and the knowledge of the methanol concentration at this interface is very valuable in predicting the methanol cross-over rate and cell performance. Besides, such knowledge can further lead to methodologies in reducing methanol crossover and enhancing fuel cell performances.

In this work, the sharp peaks in methanol cross-over flux in an operating DMFC when the cell voltage changes abruptly are systematically studied, and the methanol concentrations at the interface between the anode catalyst layer and the electrolyte membrane are obtained. The formation mechanisms for the peaks are further explored. The methanol drag coefficients at different interfacial concentrations are obtained and a linear relationship between the interfacial methanol concentration and the methanol drag coefficient is obtained directly from the experimental results. The water drag coefficient can also be obtained.

2. Experimental studies

2.1. Experimental system

The experimental system is schematically shown in Fig. 1. The fuel cell test station was manufactured by Fuel Cell Technology, Inc. A major component of the test station is the HP® 6050A system DC electronic load controller, which is capable of controlling the electrical load on the fuel cell as well as measuring its voltage versus current responses. This experimental system also provided control over anode and cathode flow rates, cell operating temperature, operating pressure, and humidification temperature for the cathode. The cathode mass flow rate was controlled and measured by a MKS® mass flow controller, and the anode flow rate was controlled and measured by a peristaltic pump by Gilson, Inc.

The experimental fuel cell consisted of two 316 stainless steel end plates, two graphite collector plates with machined serpentine flow fields, two carbon cloth diffusion layers, two catalyst layers, and an electrolyte polymer membrane. The cell was kept at a constant temperature of 70 °C through the thermal management system during all the experiments. The membrane used was Nafion® 117; the gas diffusion layer on the anode side was carbon

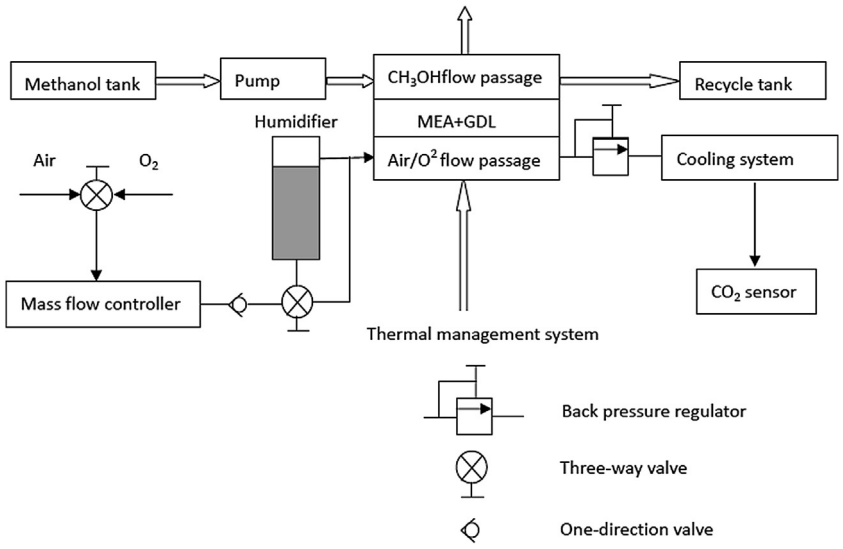

Fig. 1. Schematic of the experimental system.

cloth and ETEK ELAT® on the cathode side; the catalyst is Pt–Ru on the anode side with a loading of 4 mg cm^{-2}; and the catalyst was carbon supported Pt on the cathode side with a loading of 4 mg cm^{-2}. The total active area of the cell was 5 cm^2. The carbon dioxide sensor used was GMP221 Carbon Dioxide Probe from Vaisala Oyj, Finland. After passing through the working DMFC, the exit gas is cooled down to the room temperature of 20 °C and the carbon dioxide probe is working under this temperature.

When methanol crosses over to the cathode side, most reacts with oxygen and converts intoCO_2, and only a very small amount becomes the intermediate products CH_xO_y and CO [34]. Wang et al. [35] analyzed the chemical compositions of the cathode effluent of a DMFC with a mass spectrometer and found that the methanol crossing over the membrane to the cathode is completely oxidized to CO_2 in the presence of Pt catalyst. In this study, the flux of methanol crossover was determined by measuring the CO_2 concentration at the exit of the cathode side. The concentration of water vapor at the cathode exit was constant for each experiment since the temperature was held constant and the cathode exhaust gas was always saturated. Determining methanol crossover flux by measuring CO_2 concentration at cathode outlet is a very convenient and reliable technique [36–38]. Besides, this technique can monitor the amount of methanol crossover continuously and in real time.

2.2. Experimental methodology

In an operating DMFC, when there is no significant pressure difference between the anode and cathode sides, the methanol crossover molar flux per active area is caused by diffusion and electro-osmotic drag, thus,

$$\bar{j} = \frac{\lambda_m}{nF} I + \frac{D^{\text{eff}} \Delta C_e}{t} \tag{1}$$

where, λ_m is the methanol drag coefficient; n is the number of electronic charges per proton, $n = 1$; F is the Faraday constant, $F = 96485$ (C mol^{-1}); I is the fuel cell current density (A cm^{-2}); D^{eff} is the effective diffusion coefficient of methanol through the Nafion® electrolyte polymer membrane, t is the thickness of the membrane (m) and it is 1.8×10^{-4}m here; ΔC_e is the difference in methanol concentration across the membrane (M). The methanol drag coefficient can be expressed as $\lambda_m = \lambda_w X_{a/m}$ [39], whereλ_w is the water drag coefficient, $X_{a/m}$ is the methanol molar fraction at the interface between the anode catalyst layer and the membrane. The first term in the RHS in Eq. (1) is the methanol crossover flux due to the electro-osmotic drag and the second term is methanol crossover flux caused by the methanol concentration gradient.

Eq. (1) shows that the methanol crossover flux depends directly on the methanol concentration at the interface between the anode catalyst layer and the membrane. Assume the methanol solution is ideal, the methanol molar fraction at the interface between the anode catalyst layer and the electrolyte membrane can be calculated by,

$$X_{a/m} = \frac{C_{a/m}}{C_{a/m} + \left(1 - C_{a/m} V_m\right)/V_w} = C_{a/m} \cdot \left\{ C_{a/m} + \left(1000 - \frac{C_{a/m} * 32 * 1000}{794.45}\right) \frac{1}{18} \right\}^{-1} \tag{2}$$

where $C_{a/m}$ is the methanol concentration at the interface between the anode catalyst layer and the membrane, V_i is the molar volume of species i (either m for methanol or w for water) and the methanol density is taken to be 794.45 kg m^{-3}.

The methanol crossover flux per active area can be determined from the carbon dioxide concentration at the cathode exit by,

$$\bar{j} = \frac{Q \cdot X_{CO_2}}{\bar{v} A} \tag{3}$$

where $\bar{j}$ – methanol molar flux per active area (mmol min^{-1} cm^{-2})), A – cell active area (cm^2), here $A = 5$ cm^2, Q – cathode flow rate (sccm), X_{CO_2} – carbon dioxide molar fraction at the cathode exit (%), $\bar{v}$ – gas molar specific volume, $\bar{v} = \bar{R}T/p$, where p is pressure and $\bar{R}$ is the universal gas constant, T is the temperature in K at the location of the carbon dioxide probe.

Since a very high air flow rate is used in all the experiments (cathode stoichiometric ratio is greater than 40) and no humidification is provided on the cathode side, the cathode flow rate can be approximated by the air flow rate. Assuming methanol is oxidized immediately after crossing over to the cathode side [35], i.e. the methanol concentration at the cathode side of the membrane is assumed to be zero, we have, $\Delta C_e = C_{a/m}$. The carbon dioxide sensor

used is found to have instantaneous response to the changes of the cell voltage and this can be verified by the matching of the transient data of current density and CO_2. Note that such instantaneous responses are ensured by both the quick responses of the sensor and the fuel cell, which is small with high cathode flow rates.

From Eq. (1), it can be seen that when the cell voltage is abruptly changed to a new value, if the cell current also changes to a new value almost immediately, then the first term, the part of methanol crossover flux due to EOD changes immediately. However, at this moment, the methanol concentration at the interface between the anode catalyst layer and the membrane is still the same as at the previous cell voltage. It will take a period of time for this interface methanol concentration to reach the new equilibrium value at the new cell voltage. Therefore, at the time when the cell voltage changes abruptly to a new value, methanol crossover flux caused by the diffusion part remains the same while the part due to EOD decreases or increases immediately, and it takes some time for the total methanol crossover flux to reach the new equilibrium value.

A series of experiments have been conducted to record the responses of cell current density and methanol crossover flux when the cell voltage is changed abruptly. Cell voltage changes according to the following scheme: $V_{max} \rightarrow 0.394$ V $\rightarrow$ 0.096 V $\rightarrow$ 0.394 V $\rightarrow V_{max}$. Here V_{max} is the maximum cell voltage that can be measured in a closed circuit. In this work, V_{max} is obtained when the cell current density is 0.002 A cm^{-2}. The same experiments have been repeated for five different feeding methanol concentrations: 0.5 M, 1 M, 2 M, 3 M and 5 M.

Denoting the methanol concentration at the interface between the anode catalyst layer and the membrane as C_{m-n}, where m represents the feeding methanol concentration and n represents the fuel cell operating voltage state. The air flow rate in all the experiments is either 800 sccm or 1600 sccm. From Eqs. (1) and (3), we have,

$$C_{m-n}D^{\text{eff}} + 1.866 \times 10^{-8} I\lambda_{m-n} = 3 \times 10^{-8}\bar{j} \quad (4)$$

where C_{m-n} is the methanol concentration at the interface between the anode catalyst layer and the membrane; I is the cell current density; λ_{m-n} is the methanol drag coefficient through the membrane at the feeding methanol concentration of mM and cell voltage state of n. For simplicity, the following values are assigned to n:$n = 1$ when the cell operating voltage equals V_{max}, $n = 2$ when the cell voltage equals 0.394 V after it is decreased from V_{max}, $n = 3$ when the cell voltage equals 0.096 V, $n = 4$ when the cell voltage equals 0.394 V before it is increased to V_{max}. The methanol effective diffusion coefficient in the Nafion® electrolyte polymer membrane is taken to be $D^{\text{eff}} = 4.938 \times 10^{-10}$ m^2 s^{-1} at 70 °C [40].

3. Experimental results and discussions

3.1. Results at 0.5 M feeding methanol concentration

Fig. 2 shows the results of responses of cell current density and methanol crossover flux when the cell voltage is changed according to the scheme: $V_{max} \rightarrow 0.394$ V $\rightarrow$ 0.096 V $\rightarrow$ 0.394 V $\rightarrow V_{max}$. Here V_{max} is 0.857 V. Fig. 2 shows that when the cell voltage is decreased abruptly, the cell current density increases immediately. However, the methanol crossover flux does not decrease immediately to its new equilibrium value. Instead, an overshoot occurs and a positive peak is formed in the methanol crossover flux before it decreases to its new equilibrium level. Similarly, when the cell voltage is increased abruptly, the cell current density decreases immediately, and another overshoot occurs and a negative peak (valley) is formed in the methanol crossover flux. There are four peaks in methanol crossover flux corresponding to the four abrupt changes

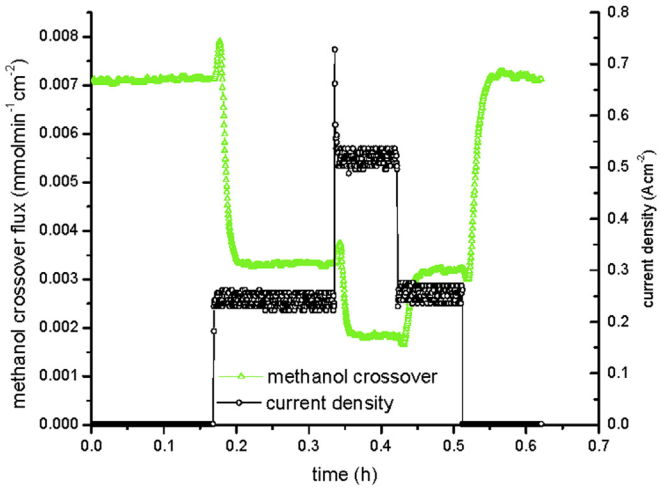

Fig. 2. Methanol crossover peaks at transient states: methanol feeding concentration 0.5 M; methanol flow rate, 3 ml min^{-1}; air flow rate, 800 sccm.

in cell voltage when all the other cell operating conditions are kept unchanged. The first peak corresponds to the cell voltage changes from V_{max} to 0.394 V; the second peak corresponds to the cell voltage changes from 0.394 V to 0.096 V; the third peak corresponds to the cell voltage changes from 0.096 V back to 0.394 V; the fourth peak corresponds to the cell voltage changes from 0.394 V back to V_{max}.

For each of these four peaks or valleys, we have one equation to describe the methanol crossover flux at the peak value. For the second peak ($I = 0.728$ A cm^{-2}, $\bar{j} = 3.487 \times 10^{-3}$ mmol min^{-1} cm^{-2}) and the fourth peak (I = 0.002 A cm^{-2}, $\bar{j} = 2.804 \times 10^{-3}$ mmol min^{-1} cm^{-2}), from Eq. (4) we have,

$$C_{0.5-2}D^{\text{eff}} + 1.358 \times 10^{-8}\lambda_{0.5-2} = 1.046 \times 10^{-10} \quad (5)$$

$$C_{0.5-4}D^{\text{eff}} + 3.731 \times 10^{-11}\lambda_{0.5-4} = 8.41 \times 10^{-11} \quad (6)$$

In these two equations, both $C_{0.5-2}$ and $C_{0.5-4}$ are the interface methanol concentration when the cell voltage is equal to 0.394 V and the methanol feeding concentration is 0.5 M, thus $C_{0.5-2} = C_{0.5-4}$. Since the methanol drag coefficient is a function of the interface methanol concentration, $\lambda = g(C_{a/m})$, then we have $\lambda_{0.5-2} = \lambda_{0.5-4}$. From Eqs. (5) and (6), we obtain,

$$\lambda_{0.5-2} = \lambda_{0.5-4} = 1.513 \times 10^{-3}, \quad \lambda_w = 0.492, \quad C_{0.5-2} = C_{0.5-4} = 0.17 \text{ M}.$$

So we are able to determine the methanol concentration at the interface between the anode catalyst layer and the membrane at 0.394 V to be 0.17 M when the feeding methanol concentration is 0.5 M. Besides, the methanol EOD coefficient is determined to be 1.513×10^{-3} under these conditions. The results show that at the cell voltage of 0.394 V, the methanol concentration at the anode catalyst layer/membrane interface is about 34% of the feeding concentration when a very low methanol concentration of 0.5 M is used.

3.2. Results at 1 M methanol concentration

Fig. 3 shows the results of responses of cell current density and methanol crossover flux when the cell voltage is changed abruptly according to the same scheme as described at 1 M feeding methanol concentration. Similarly, the first peak corresponds to the cell

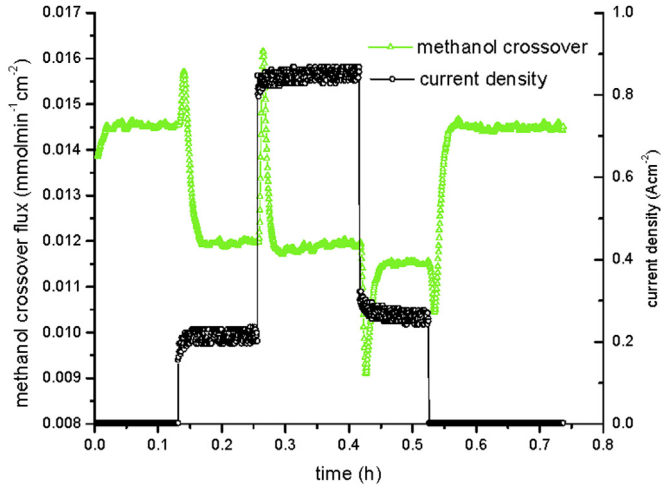

Fig. 3. Methanol crossover peaks at transient states: methanol feeding concentration 1 M; methanol flow rate, 3 ml min^{-1}; air flow rate, 800 sccm.

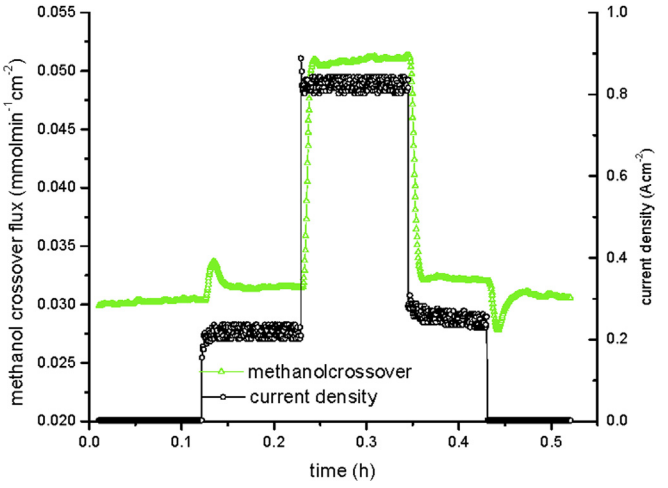

Fig. 4. Methanol crossover peaks at transient states: methanol feeding concentration 2 M; methanol flow rate, 3 ml min^{-1}; air flow rate, 800 sccm.

voltage changes from V_{max} to 0.394 V; the second peak corresponds to the cell voltage changes from 0.394 V to 0.096 V; the third peak corresponds to the cell voltage changes from 0.096 V back to 0.394 V; the fourth peak corresponds to the cell voltage changes from 0.394 V back to V_{max}. Here V_{max} equals 0.824 V.

For the second peak (I = 0.848 A cm^{-2}, $\bar{j}$ = 1.509 × 10^{-2} mmol min^{-1} cm^{-2}) and the fourth peak (I = 0.002 A cm^{-2}, $\bar{j}$ = 9.736 × 10^{-3} mmol min^{-1} cm^{-2}), from Eq. (4), we have,

$$C_{1-2}D^{eff} + 1.582 \times 10^{-8}\lambda_{1-2} = 4.526 \times 10^{-10} \quad (7)$$

$$C_{1-4}D^{eff} + 3.731 \times 10^{-11}\lambda_{1-4} = 2.921 \times 10^{-10} \quad (8)$$

Similarly, both C_{1-2} and C_{1-4} are the interface methanol concentration at cell voltage of 0.394 V when the methanol feeding concentration is 1 M, so $C_{1-2} = C_{1-4}$, $\lambda_{1-2} = \lambda_{1-4}$. Solving Eqs. (7) and (8) we have,

$$\lambda_{1-2} = 1.017 \times 10^{-2},\ \lambda_w = 0.944,\ C_{1-2} = C_{1-4} = 0.591\ \text{M}.$$

The results show that at a higher feeding methanol concentration, both the interface concentration and the EOD coefficient are higher. At 1 M feeding concentration, the methanol concentration at the anode-membrane interface is about 59% of the feeding concentration when the cell voltage is at 0.394 V. The interfacial concentration at 1 M feeding concentration is about 3.48 times of the interfacial concentration at 0.5 M feeding concentration.

3.3. Results at 2 M feeding methanol concentration

Fig. 4 shows the four peaks of methanol crossover flux when the methanol feeding concentration is 2 M. Here, V_{max} equals 0.774 V. For the second peak (I = 0.888 A cm^{-2}, $\bar{j}$ = 4.758 × 10^{-2} mmol min^{-1} cm^{-2}) and the fourth peak (I = 0.002 A cm^{-2}, $\bar{j}$ = 2.596 × 10^{-2} mmol min^{-1} cm^{-2}), from Eq. (4) we have,

$$C_{2-2}D^{eff} + 1.657 \times 10^{-8}\lambda_{2-2} = 1.427 \times 10^{-9} \quad (9)$$

$$C_{2-4}D^{eff} + 3.731 \times 10^{-11}\lambda_{2-4} = 7.789 \times 10^{-10} \quad (10)$$

Similarly both C_{2-2} and C_{2-4} are the interface methanol concentration when the methanol feeding concentration is 2 M and the cell voltage is 0.394 V, that is $C_{2-2} = C_{2-4}$ and $\lambda_{2-2} = \lambda_{2-4}$. From Eqs (9) and (10), we have

$$\lambda_{2-2} = 3.924 \times 10^{-2},\ \lambda_w = 1.336,\ C_{2-2} = C_{2-4} = 1.57\,\text{M}.$$

The interfacial concentration at 2 M feeding concentration is 1.57 M, about 9.26 times of the interface concentration at 0.5 M feeding concentration.

3.4. Results with 3 M methanol concentration

Fig. 5 shows the four peaks of methanol crossover flux when the methanol feeding concentration is 3 M and we have four equations for the four peaks. Here V_{max} equals 0.741 V. For the second peak (I = 0.856 A cm^{-2}, $\bar{j}$ = 8.298 × 10^{-2} mmol min^{-1} cm^{-2}) and the fourth peak (I = 0.002 A cm^{-2}, $\bar{j}$ = 4.461 × 10^{-2} mmol min^{-1} cm^{-2}), from Eq. (4), we have,

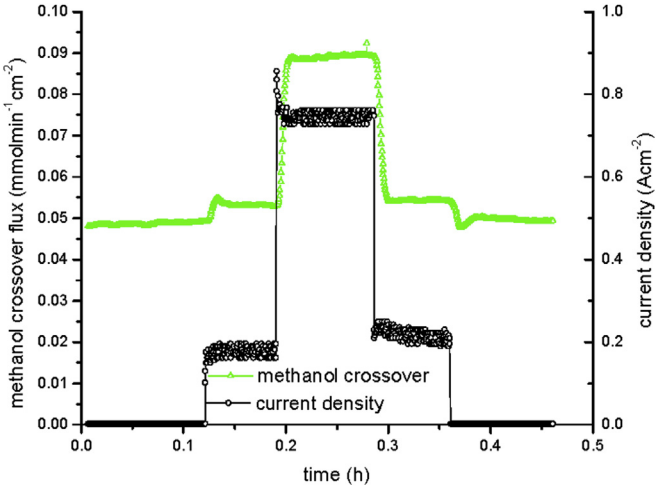

Fig. 5. Methanol crossover peaks at transient states: methanol feeding concentration 3 M; methanol flow rate, 3 ml min^{-1}; air flow rate, 1600 sccm.

Table 1
Methanol crossover peaks at transient states at cell voltage of 0.394 V. Methanol feeding concentration 0.5 ~ 5 M; methanol flow rate, 3 ml min^{-1}, air stoichiometric greater than 40(C — methanol feeding concentration, $C_{a/m}$ — interface methanol concentration, $X_{a/m}$ — interface methanol molar fraction, λ_m— methanol drag coefficient, λ_w— water drag coefficient, ΔC_a— methanol concentration differences across the anode catalyst layer, I— cell current density).

C(M)	λ_m ($\times 10^{-3}$)	$C_{a/m}$ (M)	$X_{a/m}$	I (A cm^{-2})	λ_w	Crossover flux ($\times 10^{-2}$ mmol min^{-1} cm^{-2})	ΔC_a (M)
0.5	1.513	0.1702	3.076×10^{-3}	0.23	0.492	0.321	0.33
1	10.17	0.5907	1.077×10^{-2}	0.231	0.944	1.157	0.41
2	39.24	1.5744	2.937×10^{-2}	0.236	1.336	3.207	0.43
3	72.25	2.7047	5.181×10^{-2}	0.162	1.395	5.405	0.30
5	136.2	4.6543	9.347×10^{-2}	0.11	1.457	9.134	0.35

$$C_{3-2}D^{\text{eff}} + 1.597 \times 10^{-8}\lambda_{3-2} = 2.489 \times 10^{-9} \quad (11)$$

$$C_{3-4}D^{\text{eff}} + 3.731 \times 10^{-11}\lambda_{3-4} = 1.338 \times 10^{-9} \quad (12)$$

BothC_{3-2} and C_{3-4} are the interface methanol concentration when the methanol feeding concentration is 3 M and the cell voltage is 0.394 V, that is $C_{3-2} = C_{3-4}$ and $\lambda_{3-2} = \lambda_{3-4}$. From Eqs. (11) and (12), we have

$$\lambda_{3-2} = 7.225 \times 10^{-2},\ \lambda_w = 1.395,\ C_{3-2} = C_{3-4} = 2.7\ \text{M}.$$

The interfacial methanol concentration is 2.7 M.

3.5. Results at 5 M methanol concentration

Fig. 6 shows the four peaks of methanol crossover flux when the methanol feeding concentration is 5 M and we have four equations for the four peaks. Here $V_{\max}$ equals 0.692 V. For the second peak (I = 0.696 A cm^{-2}, $\bar{j} = 1.355 \times 10^{-1}$ mmol min^{-1} cm^{-2}) and the fourth peak (I = 0.002 A cm^{-2}, $\bar{j} = 7.678 \times 10^{-2}$ mmol min^{-1} cm^{-2}), from Eq. (4), we have,

$$C_{5-2}D^{\text{eff}} + 1.298 \times 10^{-8}\lambda_{5-2} = 4.066 \times 10^{-9} \quad (13)$$

$$C_{5-4}D^{\text{eff}} + 3.731 \times 10^{-11}\lambda_{5-4} = 2.303 \times 10^{-9} \quad (14)$$

Similarly, bothC_{5-2} and C_{5-4} are the interface methanol concentration when the methanol feeding concentration is 5 M and the cell voltage is 0.394 V, that is $C_{5-2} = C_{5-4}$ and $\lambda_{5-2} = \lambda_{5-4}$. From Eqs. (13) and (14), we have

$$\lambda_{5-2} = 0.136,\ \lambda_w = 1.46\ C_{5-2} = C_{5-4} = 4.65\ \text{M}.$$

The interfacial methanol concentration is 4.65 M.

3.6. Derivation of the formula for general methanol drag coefficient

When the membrane is fully-hydrated the methanol drag coefficient is a function of only the interface methanol concentration between the anode catalyst layer and the electrolyte membrane. The summery of the values of the methanol concentrations at the interface between the anode catalyst layer and the membrane and the values of the methanol drag coefficient are listed in Table 1 at the cell voltage of 0.394 V. The methanol drag coefficient can be expressed as $\lambda_m = \lambda_w X_{a/m}$ [39], where λ_m and λ_w are the methanol and water drag coefficients, correspondingly, $X_{a/m}$ is the methanol molar fraction at the interface between the anode catalyst layer and the membrane. Assuming the methanol drag coefficient is proportional to the interfacial methanol concentration, the relationship between the methanol drag coefficient and the interfacial methanol concentration is shown in Fig. 7 and the linear fit is given by,

$$\lambda_m = bC_{a/m} \quad (15)$$

where b = 0.028. The standard deviation = 9.692×10^{-4}, and the Adjusted R-Square = 0.994.

Converting the methanol concentration to methanol molar fraction, the relationship between the methanol drag coefficient and the methanol molar fraction is shown in Fig. 8, and the linear fit is given as,

$$\lambda_m = bX_{a/m} \quad (16)$$

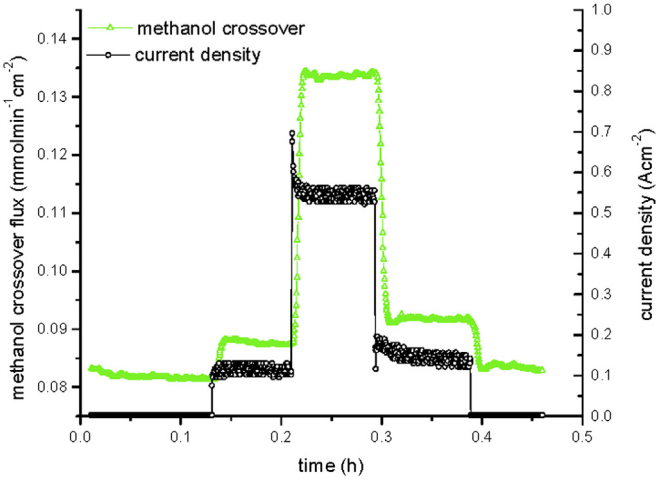

Fig. 6. Methanol crossover peaks at transient states: methanol feeding concentration 5 M; methanol flow rate, 3 ml min^{-1}; air flow rate, 1600 sccm.

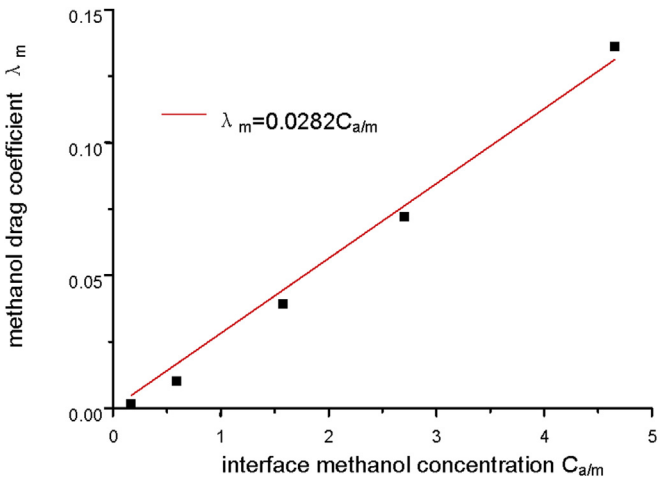

Fig. 7. Methanol drag coefficient versus methanol concentration at the interface between the anode catalyst layer and electrolyte polymer membrane.

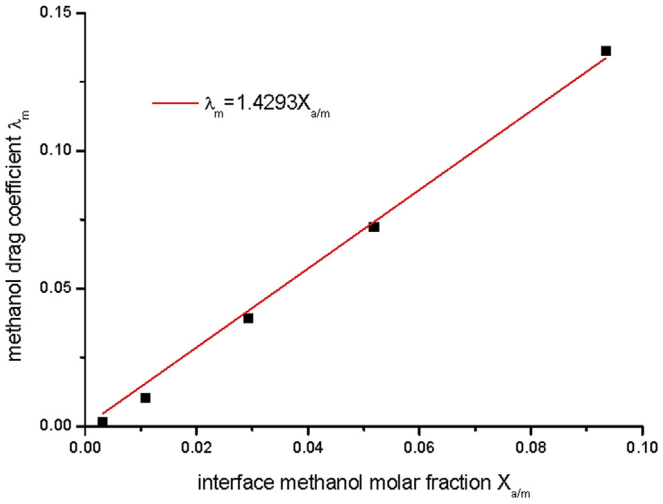

Fig. 8. Methanol drag coefficient versus methanol molar fraction at the interface between the anode catalyst layer and electrolyte polymer membrane.

where $b = 1.43$. The standard deviation = 0.033, and the Adjusted R-Square = 0.997. Comparing with the formula $\lambda_m = \lambda_w X_{a/m}$, the water drag coefficient is equal to 1.43 in general in this case. Table 1 also shows the water drag coefficients with different interface methanol concentrations, which are in agreement with those obtained in the literature [41–43]. The trend that water drag coefficient increases with the increase in methanol concentration also agrees well with the results by Schaffer et al. [44]. Note that in this work, the water drag coefficient is determined through the methanol drag coefficient, very different from the methodologies used before. Yet, such good agreements with others are obtained.

4. Conclusions

Experimental results show that sharp peaks exist in the methanol crossover flux when the cell voltage changes abruptly. From the fundamental formation mechanisms of these peaks, a novel method to determine the methanol concentration at the interface between the anode catalyst layer and the Nafion® electrolyte membrane is developed. Based on the experimental results and the analyses, the following conclusions can be made.

1) The peaks or valleys in methanol crossover flux when the cell voltage changes abruptly are caused by the different response rates of the two fundamental mechanisms of methanol crossover: diffusion and EOD.
2) The peaks or valleys in methanol crossover rate can be used to determine the interfacial methanol concentration between the anode catalyst layer and the membrane.
3) The methanol drag coefficient can be obtained from the peaks and valleys in methanol crossover rate.
4) The water drag coefficient can also be obtained from the peaks and valleys in methanol crossover rate.

Acknowledgments

The financially supports of Dorgan Fund and the NSFC (Natural Science Foundation of China) Project No.:51077096 are gratefully acknowledged.

References

[1] Jiahua Han, Hongtan Liu, J. Power Sources 164 (2007) 166–173.
[2] S.K. Kamarudin, F. Achmad, W.R.W. Daud, Int. J. Hydrogen Energy 34 (2009) 6902–6916.
[3] S.K. Kamarudin, W.R.W. Daud, S.L. Ho, U.A. Hasran, J. Power Sources 163 (2007) 743–754.
[4] T.S. Zhao, Z.X. Liang, J.B. Xu, Encyclopedia of Electrochemical Power Sources, 2009, pp. 362–369.
[5] S.R. Narayanan, A. Kindler, B. Jeffries-Nakamura, W. Chun, H. Frank, M. Smart, T.I. Valdez, S. Surampudi, G. Halpert, in: Battery Conference on Applications and Advances, 1996, p. 113.
[6] Jun-Young Park, Yongho Seo, Sangkyun Kang, Daejong You, Hyejung Cho, Youngseung Na, Int. J. Hydrogen Energy 37 (2012) 5946–5957.
[7] Huyen N. Dinh, Xiaoming Ren, Fernando H. Garzon, Piotr Zelenay, Shimshon Gottesfeld, J. Electroanal. Chem. 491 (2000) 222–233.
[8] C.K. Lin, J.F. Kuo, C.Y. Chen, J. Power Sources 187 (2009) 341–347.
[9] A.F. Ismail, N.H. Othman, A. Mustafa, J. Membr. Sci. 329 (2009) 18–29.
[10] Jatindranath Maiti, Nitul Kakati, Seok Hee Lee, Seung Hyun Jee, Young Soo Yoon, Solid State Ionics 201 (2011) 21–26.
[11] Wen Li, Arumugam Manthiram, J. Power Sources 195 (2010) 962–968.
[12] Chaiwat Yoonoo, Craig P. Dawson, Edward P.L. Roberts, Stuart M. Holmes, J. Membr. Sci. 369 (2011) 367–374.
[13] W. Li, A. Manthiram, M.D. Guiver, J. Membr. Sci. 362 (2010) 289–297.
[14] Jihoon Kim, Jae-Deok Jeon, Seung-Yeop Kwak, Microporous Mesoporous Mater. 168 (2013) 148–154.
[15] Ayokunle Omosebi, Ronald S. Besser, J. Power Sources 228 (2013) 151–158.
[16] Akiko Yamauchi, Taichi Ito, Takeo Yamaguchi, J. Power Sources 174 (2007) 170–175.
[17] Jingtao Wang, Lulu Xiao, Yuning Zhao, Hong Wu, Zhongyi Jiang, Weiqiang Hou, J. Power Sources 192 (2009) 336–343.
[18] Yang Li, Xuelin Zhang, Li Nie, Yufeng Zhang, Xiaowei Liu, J. Power Sources 245 (2014) 520–528.
[19] Namgee Jung, Yoon-Hwan Cho, Minjeh Ahn, Ju Wan Lim, Yun Sik Kang, Dong Young Chung, Jinho Kim, Yong-Hun Cho, Yung-Eun Sung, Int. J. Hydrogen Energy 36 (2011) 15731–15738.
[20] Mohammad Zhiani, Hussein Gharibi, Karim Kakaei, J. Power Sources 210 (2012) 42–46.
[21] A. Casalegno, C. Santoro, F. Rinaldi, R. Marchesi, J. Power Sources 196 (2011) 2669–2675.
[22] F.A. Halim, U.A. Hasran, M.S. Masdar, S.K. Kamarudin, W.R.W. Daud, APCBEE Procedia 3 (2012) 40–45.
[23] Wei Yuan, Yong Tang, Xiaojun Yang, Zhenping Wan, Int. J. Hydrogen Energy 37 (2012) 13510–13521.
[24] Yeong-Soo Kim, Dong-Hyun Peck, Sang-Kyung Kim, Doo-Hwan Jung, Seongyop Lim, Sung-Hyun Kim, Int. J. Hydrogen Energy 38 (2013) 7159–7168.
[25] Barbara Piela, Tim S. Olson, Plamen Atanassov, Piotr Zelenay, Electrochim. Acta 55 (2010) 7615–7621.
[26] R. Escudero-Cid, P. Hernández-Fernández, J.C. Pérez-Flores, S. Rojas, S. Garcia-Rodríguez, E. Fatás, P. Ocón, Int. J. Hydrogen Energy 37 (2012) 7119–7130.
[27] G. Jewett, Z. Guo, A. Faghri, J. Power Sources 168 (2007) 434–446.
[28] Shuangling Zhong, Xuejun Cui, Hongli Cai, Tiezhu Fu, Ke Shao, Hui Na, J. Power Sources 168 (2007) 154–161.
[29] Shuangling Zhong, Xuejun Cui, Sen Dou, Wencong Liu, J. Power Sources 195 (2010) 3990–3995.
[30] V. Baglio, A.S. Aricò, V. Antonucci, I. Nicotera, C. Oliviero, L. Coppola, P.L. Antonucci, J. Power Sources 163 (2006) 52–55.
[31] Sang Hern Seo, Chang Sik Lee, Appl. Energy 87 (2010) 2597–2604.
[32] A.S. Arico, S. Srinivasan, V. Antonucci, Fuel Cells 1 (2001) 133–161.
[33] Yu-Jen Chiu, Int. J. Hydrogen Energy 35 (2010) 6418–6430.
[34] A.S. Aricò, P. Cretì, P.L. Antoucci, V. Antonucci, Solid-State Lett. 1 (1998) 66–68.
[35] J.T. Wang, S. Wasmus, R.F. Savinell, J. Electrochem. Soc. 143 (1996) 1233.
[36] V. Gogel, T. Frey, Zhu Yongsheng, K.A. Friedrich, L. Jörissen, J. Garche, J. Power Sources 127 (2004) 172–180.
[37] S.C. Thimas, X. Ren, S. Gottesfeld, P. Zelenary, Electrochim. Acta 47 (2002) 3741–3748.
[38] S. Hikita, K. Yamane, Y. Nakajima, JSAE Rev. 22 (2001) 151–156.
[39] X. Ren, T.E. Springer, T.A. Zawodzingski, S. Gottesfeld, J. Electrochem. Soc. 147 (2000) 466–474.
[44] Thomas Schaffer, Thomas Tschinder, Viktor Hacker, Jürgen O. Besenhard, J. Power Sources 153 (2006) 210–216.
[40] Daniel T. Hallinan Jr., Yossef A. Elabd, J. Phys. Chem. B 111 (2007) 13221–13230.
[41] Qiangu Yan, Hossein Toghiani, Junxiao Wu, J. Power Sources 158 (2006) 316–325.
[42] D. Weng, J.S. Wainright, U. Landau, R.F. Savinell, J. Electrochem. Soc. 142 (1996) 1260.
[43] T. Fuller, J. Newman, J. Electrochem. Soc. 139 (1992) 1332–1337.